Earthq Sci (2013) 26(3–4):185–190
DOI 10.1007/s11589-013-0050-z

RESEARCH PAPER

Preliminary study on aftershock decay rate of the 2013 M_S7.0 Lushan earthquake

Zhe Jia · Weiwen Chen · Risheng Chu

Received: 24 October 2013 / Accepted: 2 December 2013 / Published online: 8 January 2014

Abstract We obtained a catalog of early aftershocks of the 2013 Lushan earthquake by examining waveform from a nearby station MDS which is 30.2 km far away from the epicenter, and then we analyzed the relation between aftershock rate and time. We used time-window ratio method to identify aftershocks from continuous waveform data and compare the result with the catalog provided by China Earthquake Networks Center (CENC). As expected, a significant amount of earthquakes is missing in CENC catalog in the 24 h after the main shock. Moreover, we observed a steady seismicity rate of aftershocks nearly in the first 10,000 s before an obvious power-law decay of aftershock activity. We consider this distinct early stage which does not fit the Omori law with a constant p ($p \sim 1$) value as early aftershock deficiency (EAD), as proposed by previous studies. Our study suggests that the main shock rupture process is different from aftershocks' processes, and EAD can vary in different cases as compared to earthquakes of strike-slip mechanism in California.

Keywords Aftershock rate · Early aftershock deficiency · Omori law · Earthquake rupture

Z. Jia · W. Chen
Mengcheng National Geophysical Observatory, School of Earth and Space Sciences, University of Science and Technology of China, Hefei 230026, Anhui, China

R. Chu (✉)
State Key Laboratory of Geodesy and Earth's Dynamics, Institute of Geodesy and Geophysics, CAS, Wuhan 430077, China
e-mail: chur@whigg.ac.cn

1 Introduction

Except in very limited cases that moderate earthquakes occur in isolation, most moderate intra-plate or inter-plate earthquakes are followed by numerous weaker earthquakes (Scholz 2002). Those later events are called aftershocks, which usually occur in the rupture zone of the mainshock. Some aftershocks occur well away from the mainshock, sometime referred to as off-fault aftershocks or post-shocks (Stein and Toda 2013; Li et al. 2013). Aftershocks pose a threat to efforts in mainshock rescue by inducing secondary hazards such as landslides, and further or even worsen damage to buildings which are already weakened. Thus, it is necessary to understand mechanisms of aftershock generation so that their hazard can be better mitigated. For example, promising efforts of aftershock hazard mitigation include aftershock forecasting project in California and earthquake early warning systems (Field 2011; Bakun et al. 1994; Wan et al. 2009).

The generation mechanisms of aftershocks are complicated. Aftershocks are usually thought to be caused by co-seismic slip of the mainshock, which relaxes stress concentrations from the mainshock (Scholz 2002). Static Coulomb stress has been widely adopted in explaining spatial distribution of aftershocks and proven to be quite effective (Stein 1999; King and Cocco 2001), despite with some concerns (Zhan et al. 2012). Dynamic triggering from seismic waves has also been proposed to generate aftershocks and successfully explain the decay of aftershock density versus epicentral distances (Felzer and Brodsky 2006). Besides mechanisms due to co-seismic slip of the mainshock rupture, recent studies support the hypothesis that aftershocks are driven by after-slip of the mainshock (Peng and Zhao 2009; Perfettini and Avouac 2004). As aftershocks show highly spatial and temporal clustering,

some researchers believe that aftershocks and the mainshock are different processes (Peng et al. 2006), or probably in similar processes to foreshocks which might be helpful in forecasting earthquakes (Jones 1984; Ni et al. 2010). However, some scientists propose that foreshocks, the mainshock, and aftershocks may be results from the same processes (Felzer et al. 2004). Thus, further studies are needed to resolve whether aftershocks and mainshock are the same processes or not.

Temporal behavior of aftershocks has been adopted to study relationship between the mainshock and aftershocks (Peng et al. 2006; Enescu et al. 2007). Temporal behavior of aftershocks is usually described with the Omori law, which states that aftershocks decay approximately in a rate as the inverse of time since the mainshock. However, a modified Omori law (Utsu 1961) fits the occurrence rate of aftershocks better:

$$R(t) = \frac{K}{(t+c)^p}$$

where $R(t)$ is the frequency of aftershocks in given time interval at time t after the mainshock. The exponent p has a value generally close to 1, but variable for different locations. K is the aftershock productivity depending on total number of events in the aftershock sequence, and c is the constant time shift introduced to avoid singularity when t goes to 0. Another consequence of c is that the early aftershock rate is almost constant, unlike the later aftershocks whose rate decays rapidly. Omori law with p of 1 can be predicted from the state and rate friction law (Dieterich 1992). The physical significance of c value is still under debate, mostly because it is difficult to determine early aftershock events after the main shock (Kagan 2004). Existing catalogs are usually used in previous studies on aftershock decay rate (Utsu and Ogata 1995). However, it has been known that existing catalogs are not complete for early aftershocks occurred in a short period time after the main shock, either due to overlapping of coda waves of large events or overwhelmed network analyst by too many events (Kagan 2004). To study early aftershock rate, detailed waveform analysis is usually necessary. For example, Peng et al. (2006) applied high-pass filter to waveforms to detect early aftershocks.

On April 20, 2013, a strong earthquake hit Lushan County, Sichuan Province of China. The earthquake, referred to as Lushan earthquake hereafter, caused substantial damage and fatality. According to the result from CENC, the epicenter of this earthquake is located at 30.3°E, 103.0°N. In this study, we use 24-h-long continuous waveform data of MDS station to pick out aftershocks of the Lushan mainshock (Fig. 1), and then we systematically analyze the pattern of aftershock decay rate and try to infer generation mechanism of aftershocks of Lushan.

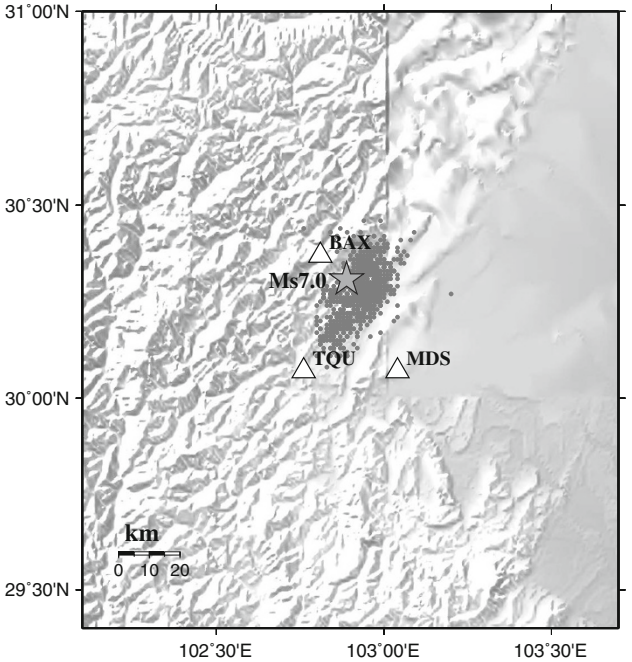

Fig. 1 The near stations BAX, MDS, and TQU (*triangle*), mainshock (*star*), and aftershocks (*dots*) of the Lushan earthquake. Aftershock locations are taken from CENC catalog. The *background* indicates relief

2 Data and analysis

Three permanent broadband seismic stations (BAX, MDS, and TQU) are within 40 km from Lushan earthquake, but only the station MDS recorded continuous waveforms after the mainshock. Station BAX stopped working for 2 days, and there were substantial data gap in TQU records. We use three component waveform data of 24-h length recorded by station MDS, located 30 km away from the epicenter of the Lushan mainshock. The sampling rate of the waveform data is 100 Hz. In order to suppress main shock coda waves to detect early aftershocks more clearly, we apply a two-pass Butterworth high-pass filter on the waveform data, following Peng et al. (2006). The corner frequency of high-pass is 5 Hz.

After the high-pass filtering, we compute the envelope of the seismograms and stack the envelope of three components to enhance the event signals. We then apply a median smoothing algorithm to each data point using a smoothing window of 0.2 s to get a smoothed envelope seismogram which is ready for identifying aftershock events (Fig. 2).

We adopt the time-window ratio method based on a phase-picking algorithm to pick out aftershock events from seismogram data (Allen 1982). In the procedure, a long time window with a short time window within is shifted through all the seismogram. We set variable dat(t) equal to the amplitude at time t, and we set variable

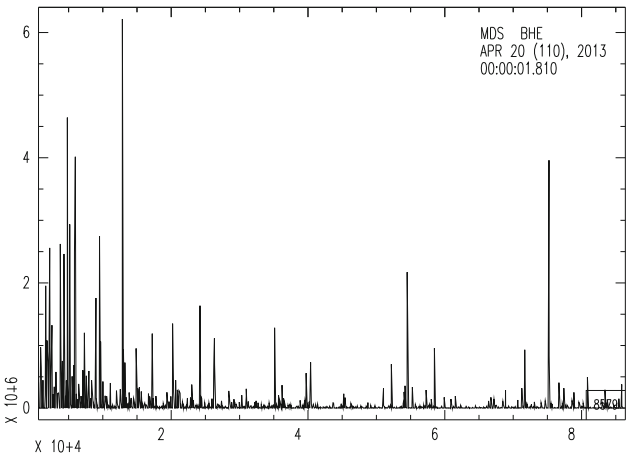

Fig. 2 High-pass-filtered and 3-component-stacked envelope seismogram recorded by station MDS for the first 24 h (86,400 s). *X-axis* indicates time by second after the origin time of the mainshock. Clearly, many significant aftershocks can be seen in 86,400 s scale

$$\mathrm{cf}(t) = \mathrm{dat}(t) \times \mathrm{dat}(t) - \mathrm{dat}(t - \mathrm{delta}) \times \mathrm{dat}(t + \mathrm{delta})$$

to describe the variation of amplitude near time t, where delta is the sampling interval of seismogram data. With the consideration of significant changes in amplitude during aftershock events, we use ratio $r(t)$ of average cf(t) in short time window to average cf(t) in long time window to pick out aftershocks. We set a threshold ratio $r_{\min}$ and then shift the long time window through the whole envelope waveform to get the ratio $r(t)$. Thus, we get aftershock events and their occurrence time where $r(t)$ is no less than threshold $r_{\min}$.

To show an example of how the process works, we select a 700–1,200 s time window of seismogram at station MDS after the Lushan main shock. We apply time-window ratio method on the data (Fig. 3), the longer time window is set to be 6 s and the shorter time window to be 2 s. We choose threshold ratio $r_{\min}$ as 2.5. During the 500-s time window, we identify 14 events. It is straightforward to observe that each significant amplitude peak in the data corresponds to peak value in the $r(t)$-t figure, which suggests the reliability of time-window ratio method in searching aftershock events.

3 Aftershock catalog comparison and seismicity rate estimation

Then, we apply the method to the 24-h seismogram since Lushan main shock. We also get earthquake catalog for the Lushan earthquake sequence from CENC data center (http://www.csndmc.ac.cn/newweb/data.htm) and then compare aftershocks identified in this study with those listed in the CENC catalog. We select events with magnitudes larger than M_L2.0 in the catalog and find a significant amount of earthquakes is missing in the CENC catalog in the 24 h after the main shock. In total, 734 aftershock events within the first 24 h are identified with our method. In contrast, only 372 events are listed in CENC catalog in this time period.

We infer that aftershocks with computed threshold value $r_{\min} = 2.5$ have magnitudes around M_L2.0. However, it is

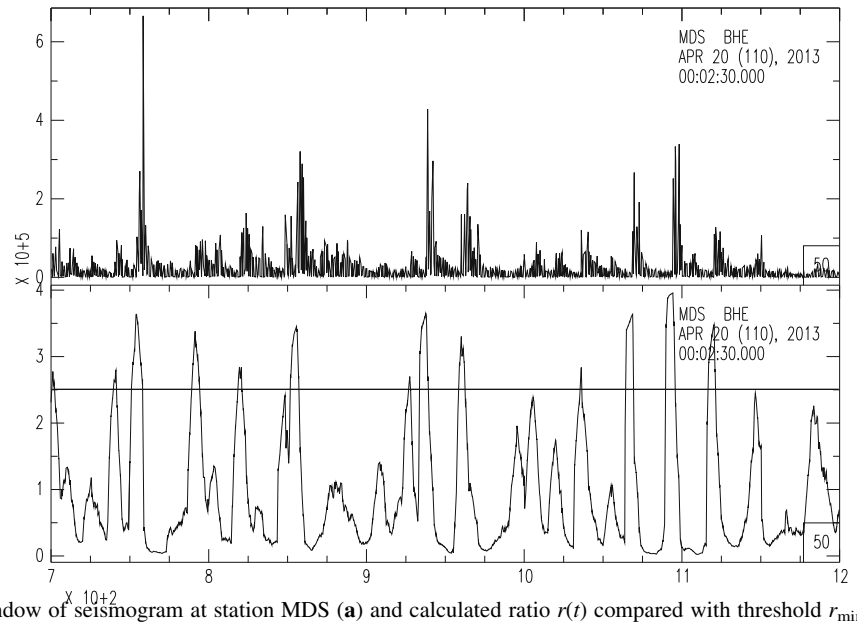

Fig. 3 A 500-s time window of seismogram at station MDS (**a**) and calculated ratio $r(t)$ compared with threshold $r_{\min} = 2.5$ (**b**). *X-axis* refers time by second after the mainshock. The *black line* in **b** means threshold ratio at 2.5. All peaks with $r(t)$ not less than 2.5 are recognized as aftershock events

difficult to determine exact magnitudes of aftershocks identified with our method, because those events are only identified on one seismic station MDS. Therefore, the comparison between the number of events provided by CENC catalog and identified in this study is just qualitative. To get a more quantitative picture of the magnitudes of the events, we compare the envelope of high-pass-filtered seismograms at MDS station with events listed in CENC catalog (Fig. 4). From this figure, it can be observed that after 10,000 s of the earthquake, events in the CENC catalog are associated with most of the spikes in the seismograms. But earlier than that, many spikes are not associated with events in the CENC catalog, suggesting that the CENC catalog is short of early aftershocks within 10,000 s since the mainshock. Particularly for the first 1,000 s, most aftershocks are missing in the catalog. But, CENC catalog includes most of the later aftershocks. It is very probable that the CENC catalog is complete 24 h after the mainshock.

According to the modified Omori law, aftershock seismicity rate in logarithm should be approximately inversely proportional to time since the main shock in logarithm. In order to study whether the aftershock rate follows modified Omori law, we compute seismicity rate by dividing in decade of time (for example, between 10^3 and 10^4) into 10 small time segments (i.e., for time window of $10^{3.0}$–$10^{3.1}$, $10^{3.1}$–$10^{3.2}$,…..,$10^{3.9}$–$10^{4.0}$ s). This choice represents a compromise between the need to have long enough intervals to achieve stability of seismicity rate and the requirement of short intervals to show the variation of seismicity. We count number of aftershocks in each small time window and calculate seismicity rate defined as number of aftershocks divided by the length of this time window.

Next, we compare the seismicity rate from envelope of station MDS with the seismicity rate calculated from CENC catalog (Fig. 5). We find that the aftershock seismicity rate of events listed in CENC catalog and events picked from envelope of MDS station match when time approximately equals 10^5 s.

Since the CENC catalog is only complete around 10^5 s after the main shock, we obtain a more complete catalog of aftershocks by adopting the early aftershocks in our study (0–8 $\times$ 10^4 s) and the aftershocks from CENC catalog (later than 8 $\times$ 10^4 s). From Fig. 5, where aftershock rate is plotted against time in logarithm–logarithm scale, we observe that the aftershock rate pattern changes obviously around 9 $\times$ 10^3 s time. Then, we apply a least square linear fitting to the exponent of the power-law decay assuming modified Omori law for time after 9 $\times$ 10^3 s time. We get a best p value as 1.23 from the fitting, and the coefficient of determination equals to 0.9813. The fact that coefficient of determination nearly equals 1 (Colin Cameron and Windmeijer 1997) suggests the seismicity rate in this time period to be following the modified Omori law very well.

However, we observe that the seismicity rate keeps approximately steady from 10^2 to 10^4 s. Noticing that seismicity rate is dominated by main shock coda wave in

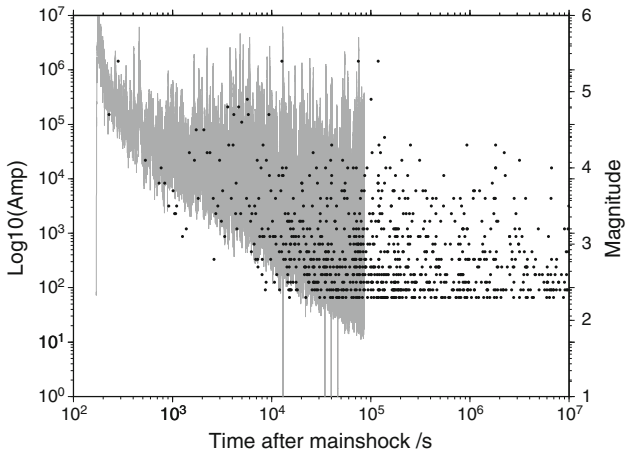

Fig. 4 Comparison between the envelopes of seismograms at station MDS with aftershock events recorded from CENC catalog. *Gray line* indicates envelope of seismograms at MDS station plotted in logarithmic time and logarithmic amplitude (labeled on the *y-axis* to the *left*). *Black points* refer to aftershock listed in CENC catalog, in which magnitudes are shown by *y-axis* to the *right*

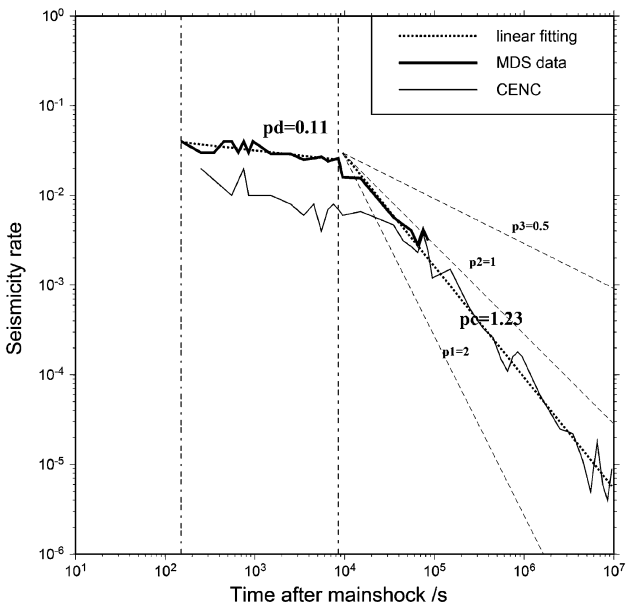

Fig. 5 Aftershock seismicity rates versus time (plotted in logarithm–logarithm scale). *Thick solid line* indicates aftershock seismicity rate from this study and *thin solid line* from events listed in CENC catalog. To facilitate comparison, we include *dash lines* showing seismicity decay rate with power of 2, 1, and 0.5, respectively. *Vertical dash-dot lines* mark boundary of early and later aftershocks. *Dotted lines* denote linear fitting of early and later aftershock decay rate

the first 150 s, we apply a least square linear fitting only for the time window of 150–8,500 s after the main shock, and get a p value that equals 0.11, significantly smaller than 1.0.

4 Discussion and conclusions

By applying high-pass filter, stacking three components of seismograms, and analyzing envelope seismograms, we were able to identify much more aftershocks despite the contamination of main shock coda wave. We find that after 8.5×10^4 s, aftershock seismicity rate follows power-law decay well, which means the aftershocks temporal behavior is well described with the modified Omori law. However, early aftershock events (before 10^4 s) are much fewer than predicted according to the modified Omori law. Instead, we observed almost steady seismicity rate from 150 to 8500 s time. Therefore, there appears to be a distinct early stage of aftershock reaction apart from the following numerous aftershocks.

Peng et al. (2006) also observed early aftershock deficiency (EAD) phenomenon in aftershock activity of 2004 M_w6.0 Parkfield earthquake. Previously, EAD indicated the transition time from main shock rupture to numerous aftershocks, and this suggests main shock rupture and its aftershock sequence to be distinct processes, also implied by results of Kagan (Kagan et al. 2005). However, in the case of Lushan main shock, the early stage with a stable seismicity appears to be much longer than previous EAD. For Lushan earthquake, the time window for EAD is about 8,000 s, but for the 2004 Parkfield earthquake, EAD duration is about 130 s. This phenomenon may be caused by a much larger magnitude of the main shock. The possible explanation is that the main shock rupture causes damages in a substantially larger volume, thus producing higher early aftershock activity.

In summary, we analyzed the seismicity rate of the Lushan earthquake and found a significant percentage of aftershocks missing in CENC catalog in the first 10^4 s after the main shock. We found that aftershock activity after 9×10^3 s fits the modified Omori law well, while we observed a fairly steady rate between time of 150 and 8,500 s. We propose this period of stage to be EAD, while the time duration of EAD is much longer than previous study. We hypothesize that the longer EAD duration is probably due to larger main shock amplitude and damage in a larger volume caused by main shock to early aftershocks. In the future, more studies involving near seismic stations are needed to investigate dependence of EAD duration upon magnitude and other earthquake source parameters.

Acknowledgments We would like to thank the editor and two anonymous reviewers. Their suggestions and comments made significant improvements to the manuscript. This work is supported by the State Key Laboratory of Geodesy and Earth's Dynamics, Institute of Geodesy and Geophysics, the Chinese Academy of Sciences through grant number SKLGED2013-7-1-Z.

References

Allen R (1982) Automatic phase pickers: their present use and future prospects. Bull Seismol Soc Am 72(6B):S225–S242

Bakun WH, Fischer FG, Jensen EG, VanSchaack J (1994) Early warning system for aftershocks. Bull Seismol Soc Am 84(2):359–365

Colin Cameron A, Windmeijer FAG (1997) An R -squared measure of goodness of fit for some common nonlinear regression models. J Econ 77(2):329–342

Dieterich JH (1992) Earthquake nucleation on faults with rate-and state-dependent strength. Tectonophysics 211(1):115–134

Enescu B, Mori J, Miyazawa M (2007) Quantifying early aftershock activity of the 2004 mid-Niigata Prefecture earthquake (M_w6.6). J Geophys Res, 112(B4):B04310

Felzer KR, Brodsky EE (2006) Decay of aftershock density with distance indicates triggering by dynamic stress. Nature 441(7094):735–738

Felzer KR, Abercrombie RE, Ekström G (2004) A common origin for aftershocks, foreshocks, and multiplets. Bull Seismol Soc Am 94(1):88–98

Field EH (2011) Aftershock statistics constitute the strongest evidence for elastic rebound in large earthquakes? Paper presented at the AGU fall meeting abstracts

Jones LM (1984) Foreshocks (1966–1980) in the San Andreas system, California. Bull Seismol Soc Am 74(4):1361–1380

Kagan YY (2004) Short-term properties of earthquake catalogs and models of earthquake source. Bull Seismol Soc Am 94(4): 1207–1228

Kagan YY, Jackson DD, Liu Z (2005) Stress and earthquakes in southern California, 1850–2004. J Geophys Res 110(B5):B05S14

King GCP, Cocco M (2001) Fault interaction by elastic stress changes: new clues from earthquake sequences. Adv Geophys 44:1–8

Li Z, Tian B, Liu S, Yang J (2013) Asperity of the 2013 Lushan earthquake in the eastern margin of Tibetan Plateau from seismic tomography and aftershock relocation. Geophys J Int 195(3):2016–2022

Ni SD, Wang WT, Li L (2010) The April 14th, 2010 Yushu earthquake, a devastating earthquake with foreshocks. Sci China Earth Sci 53(6):791–793

Peng Z, Zhao P (2009) Migration of early aftershocks following the 2004 Parkfield earthquake. Nat Geosci 2(12):877–881

Peng Z, Vidale JE, Houston H (2006) Anomalous early aftershock decay rate of the 2004 M_w6.0 Parkfield, California, earthquake. Geophys Res Lett 33(17): L17307

Perfettini H, Avouac J-P (2004) Postseismic relaxation driven by brittle creep: a possible mechanism to reconcile geodetic measurements and the decay rate of aftershocks, application to the Chi-Chi earthquake, Taiwan. J Geophys Res 109(B2):B02304

Scholz CH (2002) The mechanics of earthquakes and faulting. Cambridge university press, Cambridge

Stein RS (1999) The role of stress transfer in earthquake occurrence. Nature 402(6762):605–609

Stein RS, Toda S (2013) Megacity megaquakes—two near misses. Science 341(6148):850–852

Utsu T (1961) A statistical study on the occurrence of aftershocks. Geophys Mag 30(4):521–605

Utsu T, Ogata Y (1995) The centenary of the Omori formula for a decay law of aftershock activity. J Phys Earth 43(1):1–33

Wan K, Ni S, Zeng X, Paul S (2009) Real-time seismology for the 05/12/2008 Wenchuan earthquake of China: a retrospective view. Sci China Ser D 52(2):155–165

Zhan Z, Helmberger D, Simons M, Kanamori H, Wu W, Cubas N, Avouac J-P (2012) Anomalously steep dips of earthquakes in the 2011 Tohoku-Oki source region and possible explanations. Earth Planet Sci Lett 353:121–133